Implementation of the Functional Response in Marine Ecosystem: A State-of-the-Art Plankton Model

Anal Chatterjee and Samares Pal

1 Introduction

The study of plankton-fish interaction is one of key area in marine ecology due to its global existence and importance. Most of plankton-fish interaction dynamics are based upon classical Lotka-Volterra mechanism, in which growth of zooplankton depend on phytoplankton and zooplankton predation rate of fish is the growth rate of fish with a conversion factor.

In complex dynamics, prey species make use of refuge to allow some degree of protection of the prey from predator. This prevents the predation of the prey population to some extent. In it's absence, prey density may increase due to a simultaneous increase of refuge that will trigger population outbreaks and forms multiple stable states. Recently, the scientists carried out many outcomes by considering refuge term in prey-predator system. The author in [1] examined the global stability of a stage-structured prey-predator model in presence of prey refuge. The researchers in [2] studied that prey refuge has a positive impact on Leslie-Gower-prey-predator model.

The phytoplankton (prey) community uses refuge to protect itself from the zooplankton (predator) community. This prevents the predation of the phytoplankton population to some extent [3–6]. Some researchers are opening new areas for study by incorporating refuge in the marine plankton system. The analysis of refuge in [7] showed that it has a strong effect in a phytoplankton-zooplankton spatiotemporal dynamics system. The authors in [8] establishes the vital role played

A. Chatterjee (✉)
Department of Mathematics, Barrackpore Rastraguru Surendranath College, Kolkata, India

S. Pal
Department of Mathematics, University of Kalyani, Kalyani, India

by phytoplankton refuge and toxin on the occurrence and termination of algal blooms in freshwater lake. The authors in [9] investigated the plankton dynamics in pond and the impact of zooplankton refuge on growth of tilapia (*Oreochromis niloticus*).

There are many environmental fluctuations which are not considered in deterministic models as they do not account for the variations in random parameters [10]. In such cases, a stochastic model is a better choice as they provide a realistic view of the natural system. Stochastic model of toxic producing phytoplankton-fish are studied recently in [11] for a clear understanding of the plankton dynamics. The authors in [11, 12] investigated that high and low value of environmental fluctuations may lead to the extinction of the population as well as population weakly persistent in the mean respectively. Recently, the scientists in [13] examined that white noise can affect directly the survival of plankton population in toxin producing phytoplankton-zooplankton interaction model.

Based on the above observations, we constructed a three-dimensional model focusing on the effects of phytoplankton refuge and zooplankton refuge on the marine ecosystem. Firstly, a mathematical model is designed by considering suitable functional responses. It is assumed that as per functional response type II the grazing rate of zooplankton is dependent on the phytoplankton. Zooplankton predation by fish follows a functional response type III, and the predation rate increases in a sigmoidal way with prey density. Also, many planktivorous fish feeds on chironomids, tubifex, or other bottom dwelling invertebrates. Thus, there is chance of switching to suitable prey which results in a type-III response considering there is absence of significant time-lag [14]. Further, the roles and the interaction of both plankton species and refuge phytoplankton and zooplankton are studied.

The paper is organized as follows. After the above introductory section, we move onto the model construction and the analysis of the deterministic model in Sect. 2 and Sect. 3 respectively. The stochastic counterpart is presented next, results on the numerical simulations are reported in Sect. 5 and discussed in the final section.

2 The Mathematical Model

Let P, Z and F be the concentration of the phytoplankton, zooplankton and fish population at time t with carrying capacity K and constant intrinsic growth rate r. Here α_1 and α_2 be the maximal zooplankton ingestion rate and conversion rate for the growth of zooplankton respectively ($\alpha_2 \leq \alpha_1$). Also, let γ_1 and γ_2 be the maximal planktivorous fish ingestion rate and conversion rate due to grazing of herbivorous zooplankton ($\gamma_2 \leq \gamma_1$). Further, d_1 and d_2 represent the mortality rates of the zooplankton and planktivorous fish biomass respectively. Let h be the harvesting rate of planktivorous fish population. We consider Holling type II and Holling III functional forms to illustrate the grazing phenomena with K_1 and K_2 as half saturation constants. We consider $m \in [0, 1)$ and $n \in [0, 1)$ are constant measures of the degree or strength of phytoplankton refuge and zooplankton refuge respectively.

With these above biological assumptions our model system is [15]

$$
\left.\begin{aligned}
\frac{dP}{dt} &= rP(1 - \frac{P}{K}) - \frac{\alpha_1(1-m)PZ}{K_1 + (1-m)P} \equiv G_1(P, Z, F) \\
\frac{dZ}{dt} &= \frac{\alpha_2(1-m)PZ}{K_1 + (1-m)P} - \frac{\gamma_1(1-n)^2 Z^2 F}{K_2 + (1-n)^2 Z^2} - d_1 Z \equiv G_2(P, Z, F) \\
\frac{dF}{dt} &= \frac{\gamma_2(1-n)^2 Z^2 F}{K_2 + (1-n)^2 Z^2} - (d_2 + h)F \equiv G_3(P, Z, F)
\end{aligned}\right\} \qquad (1)
$$

Firstly, we analyzed the system (1) with the following initial conditions,

$$
P(0) > 0, \ Z(0) > 0, \ F(0) > 0. \qquad (2)
$$

Explicitly, the jacobian matrix at $\overline{E} = (\overline{P}, \overline{Z}, \overline{F})$ can be illustrate as

$$
\overline{V} =
\begin{bmatrix}
r - \frac{2r\overline{P}}{K} - \frac{K_1\alpha_1(1-m)\overline{Z}}{[k_1+(1-m)\overline{P}]^2} & -\frac{\alpha_1(1-m)\overline{P}}{K_1+(1-m)\overline{P}} & 0 \\
\frac{K_1\alpha_2(1-m)\overline{Z}}{[K_1+(1-m)\overline{P}]^2} & \frac{\alpha_2(1-m)\overline{P}}{K_1+(1-m)\overline{P}} - \frac{2\gamma_1 K_2(1-n)^2\overline{Z}\ \overline{F}}{[K_2+(1-n)^2\overline{Z}^2]^2} - d_1 & -\frac{\gamma_1(1-n)^2\overline{Z}^2}{K_2+(1-n)^2\overline{Z}^2} \\
0 & \frac{2\gamma_2 K_2(1-n)^2\overline{Z}\ \overline{F}}{[K_2+(1-n)^2\overline{Z}^2]^2} & \frac{\gamma_2(1-n)^2\overline{Z}^2}{K_2+(1-n)^2\overline{Z}^2} - (d_2+h)
\end{bmatrix}.
$$
$$(3)$$

3 Some Preliminary Results

3.1 Positive Invariance

By setting $X = (P, Z, F)^T \in \mathbf{R}^3$ and $G(X) = [G_1(X), G_2(X), G_3(X)]^T$, with $G : \mathbf{R}_+^3 \to \mathbf{R}^3$ and $G \in C^\infty(\mathbf{R}^3)$, Eq. (1) becomes

$$
\dot{X} = J(X), \qquad (4)
$$

together with $X(0) = (P(0), Z(0), F(0)) = (X_1, X_2, X_3) = X_0 \in \mathbf{R}_+^3$. It is easy to check that whenever $X(0) \in \mathbf{R}_+^3$ with $X_i = 0$, for i=1, 2, 3, then $G_i(X)|_{X_i=0} \geq 0$. Then any solution of equation (4) with $X_0 \in \mathbf{R}_+^3$, say $X(t) = X(t; X_0)$, is such that $X(t) \in \mathbf{R}_+^3$ for all $t > 0$.

3.2 Equilibria

The system (1) possesses the following four equilibria: plankton free equilibrium $E_0 = (0, 0, 0)$ and zooplankton free equilibrium $E_{01} = (K, 0, 0)$, fish free equilibrium $E_1(P_1, Z_1, 0)$ and coexistence equilibrium $E^* = (P^*, Z^*, F^*)$.

3.2.1 Plankton Free Equilibrium

E_0 is always feasible. The eigenvalues evaluate from (3) at E_0 are $r > 0$, $-d_1 < 0$ and $-(d_2 + h)$. Thus, it is clearly indicates that E_0 is always unstable.

3.2.2 Zooplankton Free Equilibrium

E_{01} is always feasible. The eigenvalues evaluate from (3) at E_{01} are $-r$, $-(d_2 + h)$ and $\frac{\alpha_2(1-m)K}{K_1+(1-m)K} - d_1$. Therefore, E_{01} is asymptotically stable if

$$m > \frac{K\alpha_2 - d_1(K + K_1)}{K(\alpha_2 - d_1)} \tag{5}$$

hold.

3.2.3 Fish Free Equilibrium

The population level at $E_1(P_1, Z_1, 0)$ are $P_1 = \frac{K_1 d_1}{(\alpha_2 - d_1)(1-m)}$ and $Z_1 = \frac{r K_1 \alpha_2 [K(\alpha_2 - d_1)(1-m) - K_1 d_1]}{\alpha_1 K(1-m)^2(\alpha_2 - d_1)^2}$. Feasibility at E_1 exists if $\alpha_2 > d_1$ and $m < \frac{K\alpha_2 - d_1(K+K_1)}{K(\alpha_2 - d_1)}$. By factorizing jacobian (3) at E_1 gives one explicit eigenvalue $\frac{\gamma_2(1-n)^2 Z_1^2}{K_2+(1-n)^2 Z_1^2} - (d_2+h)$ and the quadratic equation $\lambda^2 + P_1 \left(\frac{r}{K} - \frac{\alpha_1(1-m)Z_1}{[K_1+(1-m)P_1]^2} \right) \lambda + \frac{\alpha_1 \alpha_2 K_1(1-m)^2 P_1 Z_1}{[K_1+(1-m)P_1]^3} = 0$. Clearly, two roots are negative real parts at E_1. Therefore, stability of E_1 is ensured by

$$R_0 = \frac{\gamma_2(1-n)^2 Z_1^2}{(d_2+h)[K_2 + (1-n)^2 Z_1^2]} < 1. \tag{6}$$

3.2.4 Coexistence Equilibrium

The coexistence equilibrium at $E^* = (P^*, Z^*, F^*)$ are $Z^* = \frac{1}{(1-n)}\sqrt{\frac{(\mu_2+h)K_2}{[\gamma_2-(\mu_2+h)]}} = q$ while F^* is ensured by solving $\frac{[K_2\gamma_2(\alpha_2-d_1)(1-m)P^*-d_1 K_1]}{[K_1+(1-m)P^*]\gamma_1(1-n)q[\gamma_2-(\mu_2+h)]}$ and $P^* = \frac{B+\sqrt{B^2+4AC}}{2A}$ which is ensured from equation $AP^* - BP^* - C = 0$ where $A = rK(1-m)$, $B = [rK(1-m) - rK_1]$ and $C = [rKK_1 - K\alpha_1(1-m)q]$.

At E^*, the jacobian matrix of system (1) can be written as

$$V^* = \begin{bmatrix} a_{11} & a_{12} & 0 \\ a_{21} & a_{22} & a_{23} \\ 0 & a_{32} & 0 \end{bmatrix},$$

where $a_{11} = \frac{\alpha_1(1-m)P^*Z^*}{[K_1+(1-m)P^*]^2} - \frac{rP^*}{K} < 0,\ a_{12} = -\frac{\alpha_1(1-m)P^*}{K_1+(1-m)P^*} < 0, a_{21} = \frac{K_1\alpha_2(1-m)Z^*}{[K_1+(1-m)P^*]^2} > 0,\ a_{22} = \frac{\gamma_1(1-n)^2Z^*F^*}{K_2+(1-n)^2Z^{*2}} - \frac{2\gamma_1K_2Z^*F^*}{K_2+(1-n)^2Z^{*2}} \in \mathbf{R},\ a_{23} = -\frac{\gamma_1(1-n)^2Z^{*2}}{K_2+(1-n)^2Z^{*2}} < 0,\ a_{32} = \frac{2\gamma_2K_2(1-n)^2Z^*F^*}{[K_2+(1-n)^2Z^{*2}]^2} > 0$.

The characteristic equation is

$$y^3 + Q_1y^2 + Q_2y + Q_3 = 0 \tag{7}$$

where $Q_1 = -(a_{11} + a_{22})$, $Q_2 = a_{11}a_{22} - a_{12}a_{21} - a_{23}a_{32}$; $Q_3 = a_{11}a_{23}a_{32}$. By the Routh-Hurwitz criteria, all roots of above equation have negative real parts if and only if $Q_i > 0$, and $Q_1Q_2 - Q_3 > 0, i = 1, 2, 3$.

Here we consider two cases depending on the sign of a_{22}.

Case 1 When $a_{22>0}$, then $Q_1 > 0$ if $\frac{rP^*}{K} - \frac{\alpha_1(1-m)P^*Z^*}{[K_1+(1-m)P^*]^2} > \frac{\gamma_1(1-n)^2Z^*F^*}{K_2+(1-n)^2Z^{*2}} - \frac{2\gamma_1K_2Z^*F^*}{K_2+(1-n)^2Z^{*2}}$. Also, $Q_2 > 0$ if $-a_{12}a_{21} > -a_{11}a_{22} + a_{23}a_{32}$ since $a_{11}a_{22} < 0$, $a_{12}a_{21} < 0$ and $a_{23}a_{32} < 0$.

Here, clearly $Q_3 = a_{32}a_{11}a_{23} > 0$.

Case 2 When $a_{22<0}$ which indicates $Q_1 > 0$ and $Q_2 > 0$ if $a_{11}a_{22} > a_{12}a_{21} + a_{23}a_{32}$ and obviously, $Q_3 > 0$.

In addition, according to Routh-Hurwitz criterion, $Q_1Q_2 - Q_3 > 0$ must be satisfied if $Q_1Q_2 > Q_3$ which indicates that the system becomes locally asymptotically stable at E^* depending upon system parameters.

Remark 1 The system produces a Hopf-bifurcation at the coexistence equilibrium if the following two conditions are satisfied,

$$Q_1(n_c)Q_2(n_c) - Q_3(n_c) = 0, \quad Q_1'(n_c)Q_2(n_c) + Q_1(n_c)Q_2'(n_c) - Q_3'(n_c) \neq 0. \tag{8}$$

3.3 Hopf Bifurcation at Coexistence

Let us consider a value $n = n_c$ such that $Q_1(n_c)Q_2(n_c) - Q_3(n_c) = 0$. Then at $n = n_c$ the characteristic equation (7) becomes $(\rho + Q_1)(\rho^2 + Q_2) = 0$. Clearly the equation has three roots which are $\pm\sqrt{Q_2}i$ and $-Q_1$ i.e. two roots are pair of purely complex roots and third roots is negative. To examine the transversality condition, let us consider any point n of ϵ-neighborhood of n_c where $\rho_{1,2} = a(n) \pm ib(n)$. Putting this in (7) and separate the real and imaginary parts we get the following results:

$$a^3 - 3ab^2 + p_1(a^2 - b^2) + p_2a + p_3 = 0 \tag{9}$$

$$(3a^2b - b^3) + 2p_1ab + p_2 = 0 \tag{10}$$

Since $b(n) \neq 0$, then from (10) we have $b^2 = 3a^2 + 2Q_1a + Q_2$.
Putting the value of b^2 in (7) we have

$$8a^3 + 8Q_1a^2 + 2a(Q_1^2 + Q_2) + Q_1Q_2 - Q_3 = 0. \tag{11}$$

Now differentiating w.r.t n at $n = n_c$ we get the following results
$\left[\frac{da}{dn}\right]_{n=n_c} = -\left[\frac{1}{2(Q_1^2 + Q_2)}\frac{d}{dn}(Q_1Q_2 - Q_3)\right]_{n=n_c} \neq 0$ provided $\left[\frac{d}{dn}(Q_1Q_2 - Q_3)\right]_{n=n_c} \neq 0$ i.e. second condition of (8).

4   The Stochastic Model

Here, we study our system based on the environmental parameters and their fluctuations. All the parameters are assumed to be constant with time t. The stochastic stability of the coexistence equilibrium is tested.

A deterministic system can be extended to stochastic system by two process. Firstly, by replacing one of the environmental parameters by some random parameters and secondly, without changing any particular parameter in deterministic equations and including a randomly fluctuating driving force [16].

Here we choose the second method. The Gaussian white noise type stochastic perturbations of the state variables around their steady values E^* is very effective to model rapidly fluctuating phenomena which are proportional to the distances P, Z, F of each population from their equilibrium value P^*, Z^*, F^* [17]. Based on above assumption, the deterministic system (1) can be extended to the following stochastic model

$$
\begin{aligned}
dP &= G_1(P, Z, F)dt + \sigma_1(P - P^*)d\xi_t^1, \\
dZ &= G_2(P, Z, F)dt + \sigma_2(Z - Z^*)d\xi_t^2, \\
dF &= G_3(P, Z, F)dt + \sigma_3(F - F^*)d\xi_t^3
\end{aligned}
\tag{12}
$$

in which real constant parameters σ_1, σ_2 and σ_3 are considered to be the intensities of environmental fluctuations and $\xi_t^i = \xi_i(t)$, $i = 1, 2, 3$ to be the standard Wiener processes independent of each other [18].

The stochastic system (12) can be written in compact form like an Itō stochastic differential system

$$dX_t = G(t, X_t)dt + g(t, X_t)d\xi_t, \quad X_{t0} = X_0, \tag{13}$$

where the solution of above equation $X_t = (P, Z, F)^T$, for $t > 0$ is known as Itō process. Here G is the drift coefficient or it can be written as slowly varying continuous component. The diffusion coefficient is represented by $g = \text{diag}[\sigma_1(P - P^*), \sigma_2(Z - Z^*), \sigma_3(F - F^*)]$ of the diagonal matrix which can expressed by the rapidly varying continuous random component. $\xi_t = (\xi_t^1, \xi_t^2, \xi_t^3)^T$ can be considered as a three-dimensional stochastic process having scalar Wiener process components with increments $\Delta \xi_t^j = \xi_j(t + \Delta t) - \xi_j(t)$ which are independent Gaussian random variables $\mathbf{N}(0, \Delta t)$. The system (12) is known as multiplicative noise as the diffusion matrix g depends upon the solution of X_t.

4.1 Stochastic Stability of the Coexistence Equilibrium

The stochastic differential system (12) can be centered at its coexistence equilibrium E^* by introducing the perturbation vector $U(t) = (u_1(t), u_2(t), u_3(t))^T$, with $u_1 = P - P^*$, $u_2 = Z - Z^*$, $u_3 = F - F^*$. To derive the asymptotic stability in the mean square sense by the Lyapunov functions method, working on the complete nonlinear equations (12), could be attempted, following [19]. But for simplicity we deal with the stochastic differential equations obtained by linearizing (12) about the coexistence equilibrium E^*. The linearized version of (13) around E^* is given by

$$dU(t) = F_L(U(t))dt + g(U(t))d\xi(t), \tag{14}$$

where now $g(U(t)) = \text{diag}[\sigma_1 u_1, \sigma_2 u_2, \sigma_3 u_3]$ and

$$F_L(U(t)) = \begin{bmatrix} a_{11}u_1 + a_{12}u_2 + a_{13}u_3 \\ a_{21}u_1 + a_{22}u_2 + a_{23}u_3 \\ a_{31}u_1 + a_{32}u_2 + a_{33}u_3 \end{bmatrix} = MU,$$

and the coexistence equilibrium corresponds now to the origin $(u_1, u_2, u_3) = (0, 0, 0)$. Let $\Omega = [(t \geq t_0) \times R^3, t_0 \in R^+]$ and let $\Theta(t, X) \in C^{(1,2)}(\Omega)$ be a differentiable function of time t and twice differentiable function of X. Let further

$$L_\Theta(t, u) = \frac{\partial \Theta(t, u(t))}{\partial t} + f^T(u(t)) \frac{\partial \Theta(t, u)}{\partial u} + \frac{1}{2} \text{tr} \left[g^T(u(t)) \frac{\partial^2 \Theta(t, u)}{\partial u^2} g(u(t)) \right], \tag{15}$$

where

$$\frac{\partial \Theta}{\partial u} = \left(\frac{\partial \Theta}{\partial u_1}, \frac{\partial \Theta}{\partial u_2}, \frac{\partial \Theta}{\partial u_3} \right)^T, \quad \frac{\partial^2 \Theta(t, u)}{\partial u^2} = \left(\frac{\partial^2 \Theta}{\partial u_j \partial u_i} \right)_{i,j=1,2,3}.$$

With these positions, we now recall the following result, [20].

Theorem 1 *Assume that the functions $\Theta(U, t) \in C_3(\Omega)$ and L_Θ satisfy the inequalities*

$$r_1|U|^\beta \leq \Theta(U, t) \leq r_2|U|^\beta, \tag{16}$$

$$L_\Theta(U, t) \leq -r_3|U|^\beta, \quad r_i > 0, \ \ i = 1, 2, 3, \ \ \beta > 0. \tag{17}$$

Then the trivial solution of (14) is exponentially β-stable for all time $t \geq 0$.

Remark 2 For $\beta = 2$ in (16) and (17), the trivial solution of (14) is exponentially mean square stable; furthermore, the trivial solution of (14) is globally asymptotically stable in probability [20].

Theorem 2 *Assume $a_{ij} < 0$, $i, j = 1, 2, 3$, and that for some positive real values of ω_k, $k = 1, 2$, the following inequality holds*

$$\left[2(1 + \omega_2)a_{22} + 2a_{32}\omega_2 + (1 + \omega_2)\sigma_2^2\right]\left[2a_{23}\omega_2 + (\omega_1 + \omega_2)\sigma_3^2\right]$$

$$> [a_{12}\omega_1 + a_{22}\omega_2 + a_{23}(1 + \omega_2) + a_{32}(\omega_1 + \omega_2)]^2. \tag{18}$$

Then if $\sigma_1^2 < -2a_{11}$, it follows that

$$\sigma_2^2 < -\frac{2a_{22}(1 + \omega_2) + 2a_{32}\omega_2}{1 + \omega_2}, \quad \sigma_3^2 < -\frac{2a_{23}\omega_2}{\omega_1 + \omega_2}, \tag{19}$$

where

$$\omega_1{}^* = \frac{a_{21}}{a_{11} - a_{12} - a_{32}}, \quad \omega_2{}^* = \frac{a_{11}}{a_{12} - a_{11} + a_{32}}, \quad a_{22} < 0. \tag{20}$$

and the zero solution of system (12) is asymptotically mean square stable.

Proof We consider the Lyapunov function

$$\Theta(u(t)) = \frac{1}{2}\left[\omega_1(u_1 + u_3)^2 + u_2{}^2 + \omega_2(u_2 + u_3)^2\right],$$

where real positive constants ω_1 and ω_2 to be define later.

It is straightforward to verify that inequalities (16) are valid for $\beta = 2$. Moreover,

$$L_\Theta(u(t)) = a_{11}\omega_1 u_1^2 + [a_{22}(1 + \omega_2) + a_{32}\omega_2]\, u_2^2 + [a_{23}\omega_2]\, u_3^2$$

$$+ u_1 u_2\, [a_{12}\omega_1 + a_{21}(1 + \omega_2) + a_{32}\omega_1] + u_2 u_3\, [a_{12}\omega_1 + a_{22}\omega_2 + a_{23}(1 + \omega_2)$$

$$+ a_{32}(\omega_1 + \omega_2)] + u_3 u_1\, [a_{11}\omega_1 + a_{21}\omega_2]$$

$$+ \frac{1}{2}\mathrm{tr}\left[g^T(u(t))\frac{\partial^2 \Theta}{\partial u^2}g(u(t))\right].$$

Now we evaluate that

$$\frac{\partial^2 \Theta}{\partial u^2} = \begin{vmatrix} \omega_1 & 0 & \omega_1 \\ 0 & 1 + \omega_2 & \omega_2 \\ \omega_1 & \omega_2 & \omega_1 + \omega_2 \end{vmatrix},$$

so that we can estimate the trace term as

$$\text{tr}\left[g^T(u(t)) \frac{\partial^2 \Theta}{\partial u^2} g(u(t)) \right] = \omega_1 {\sigma_1}^2 {u_1}^2 + (1 + \omega_2){\sigma_2}^2 {u_2}^2 + (\omega_1 + \omega_2){\sigma_3}^2 {u_3}^2.$$

Introducing (20), the Lyapunov function turn into $L_\Theta(u(t)) = -u^T Q u$, where Q be the real symmetric matrix

$$Q = \begin{vmatrix} -a_{11}\omega_1 - \frac{1}{2}\omega_1\sigma_1^2 & 0 & 0 \\ 0 & -(1 + \omega_2)a_{22} - \omega_2 a_{32} - \frac{1}{2}(1 + \omega_2)\sigma_2^2 & Q_{23} \\ 0 & Q_{23} & Q_{33} \end{vmatrix}$$

where

$$Q_{23} = -\frac{a_{12}\omega_1 + a_{22}\omega_2 + a_{23}(1 + \omega_2) + a_{32}(\omega_1 + \omega_2)}{2}$$

and $Q_{33} = -a_{23}\omega_2 - \frac{1}{2}(\omega_1 + \omega_2)\sigma_3^2$. Easily, the inequality $L_\Theta(u(t)) \leq -u^T Q u$ holds. On the other hand, (18) and (19) imply that Q is positive definite and therefore all its eigenvalues $\lambda_i(Q)$, $i = 1, 2, 3$, are positive real numbers. Let $\lambda_m = \min\{\lambda_i(Q), i = 1, 2, 3\} > 0$. From the previous inequality for $L_\Theta(u(t))$ we thus get

$$L_\Theta(u(t)) \leq -\lambda_m |u(t)|^2,$$

thus completing the proof.

Remark 3 Theorem 2 provides the necessary conditions for the stochastic stability of the coexistence equilibrium E^* under environmental fluctuations, [21]. Thus the internal parameters of the model together with the intensities of the environmental fluctuations help in maintaining the stability of the stochastic system.

5 Numerical Simulations

In this section, we undergo the analysis of the dynamic characteristics of plankton-fish species with the help of numerical simulations. We begin with a reference set of parametric values (cf. Table 1, [22]) in which the criterion for existence at $E^* =$

Table 1 A set of parametric values

Parameter	Definition	Default value
r	Constant intrinsic growth rate of phytoplankton	8
K	Carrying capacity of phytoplankton	1.5
α_1	Maximal zooplankton ingestion rate	2
α_2	Maximal zooplankton conversion rate	1.5
β_1	Maximal fish ingestion rate	1
β_2	Maximal fish conversion rate	0.6
d_1	Mortality rate of zooplankton	0.3
d_2	Mortality rate of fish	0.36
h	Harvesting rate of fish	0.015
K_1	Half saturation constant for phytoplankton	0.5
K_2	Half saturation constant for zooplankton	1
m	Measures of the degree or strength of phytoplankton refuge	0.4
n	Measures of the degree or strength of zooplankton refuge	0.35

(1.20, 1.97, 1.78) is satisfied and coexistence equilibrium is locally asymptotically stable (cf. Fig. 1a). Now by varying the different parametric values we study the dynamic behavior of system (1).

5.1 Effects of n

If the value of strength of zooplankton refuge $n = 0.3$ is increased, the system exhibits oscillations around E^*. But high value of $n = 0.8$, the system switches to oscillatory behavior around zooplankton free equilibrium E_1 (cf. Fig. 1b). Figures 2a–c depicts the different steady state behaviors of phytoplankton, zooplankton and fish population in the system (1) for the parameter n. Here, we see two Hopf bifurcation points at $n_c = 0.3211$ and 0.6442 (denoted by a red star (H)) with first Lyapunov coefficient being $-6.351217e^{-02}$ and $2.715545e^{01}$ which indicates that a stable and unstable limit cycle bifurcates from the H and loses its stability respectively. Here $n = 0.6443$ (LP) and $n = 0.6441$ (BP) denotes the limit point and branch point of the system (1) respectively where fish population goes to extinction. Further, we have plotted a family of limit cycles bifurcates from H points (cf. Fig. 2d).

5.2 Effects of m

Taking $m = 0.8$, the system exhibits oscillations around E^* (cf. Fig. 1c). Figures 3a–c illustrate the different steady state behaviour of each species in the system (1)
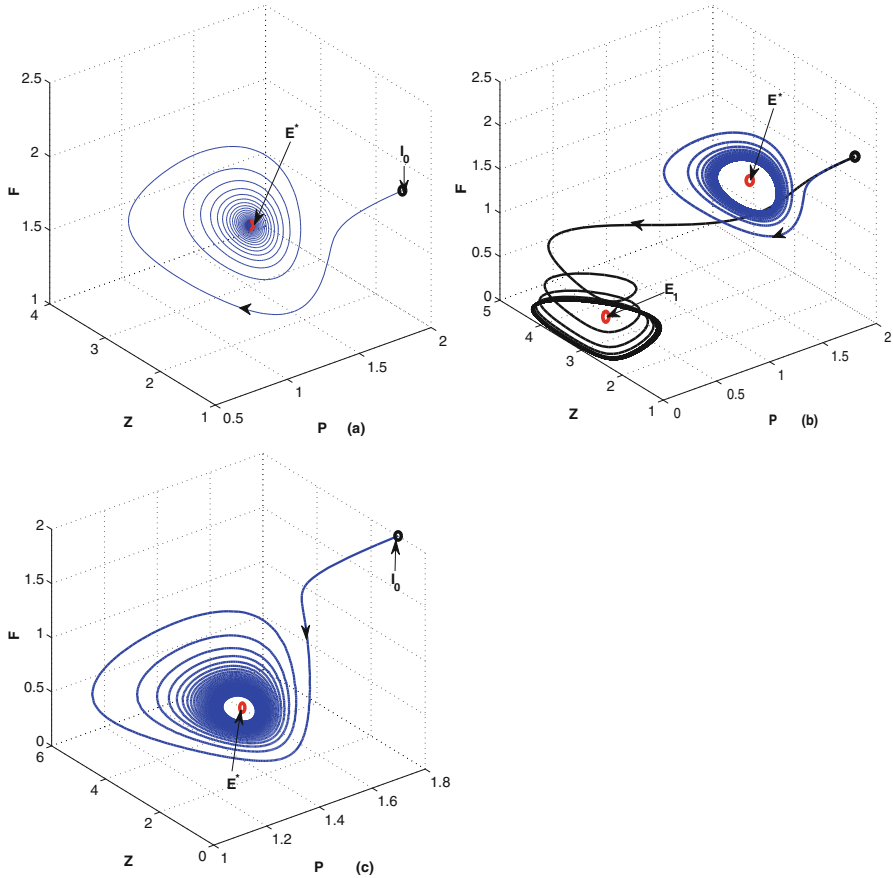
Fig. 1 (a) The equilibrium point E^* is stable for the parametric values as given in the Table 1. (b) The figure depicts oscillatory behavior around coexistence equilibrium point E^* of system (1) for $n = 0.3$ (blue line), zooplankton free equilibrium E_1 for $n = 0.8$ (black line) respectively. (c) The figure depicts oscillatory behavior around E^* of system (1) for $n = 0.8$ (blue line)

for the parameter m. Here, we see two Hopf bifurcation points at $m_c = 0.6069$ and 0.8021 (denoted by a red star (H)) with first Lyapunov coefficient being $-3.370275e^{-02}$ and $-1.339074e^{-02}$ which indicates that two stable limit cycle bifurcates from the H and loses its stability respectively. Here $m = 0.9102$ (BP) denotes branch point of the system (1). Further, we have displayed a family of limit cycles bifurcates from H points (cf. Fig. 3d).
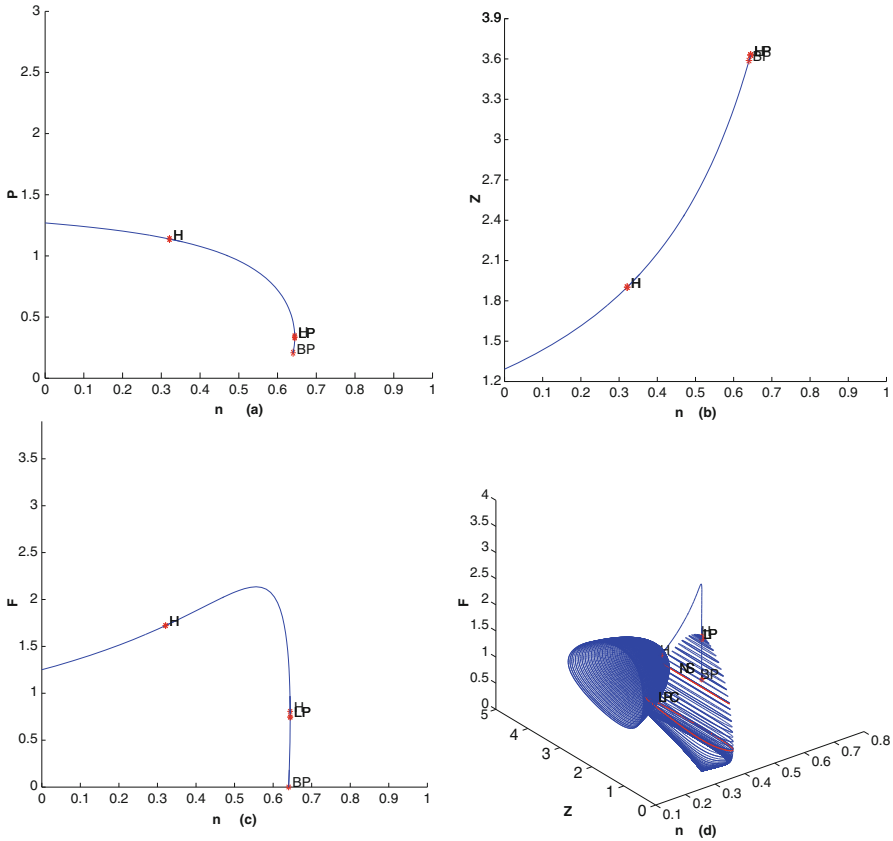
Fig. 2 (**a**) The figure depicts different steady-state behaviors of phytoplankton for the effect of *n*.
(**b**) The figure depicts different steady-state behaviors of zooplankton for the effect of *n*. (**c**) The
figure depicts different steady-state behaviors of fish for the effect of *n*. (**d**) The family of limit
cycles bifurcate from the Hopf point *H* for *n* in (n,Z,F) space

5.3 *Effects of r*

From Figs. 4a–c it follows the system (1) has two Hopf bifurcation points at
$r_c = 8.3570$ and 4.3791 with first Lyapunov coefficient being $-5.840029e^{-02}$
and $1.491169e^{+01}$, one limit point at 4.3776 and branch point at 4.4284 when we
consider constant intrinsic growth rate of phytoplankton, i.e. *r* as a free parameter.
To proceed further, a family of stable and unstable limit cycles bifurcating from
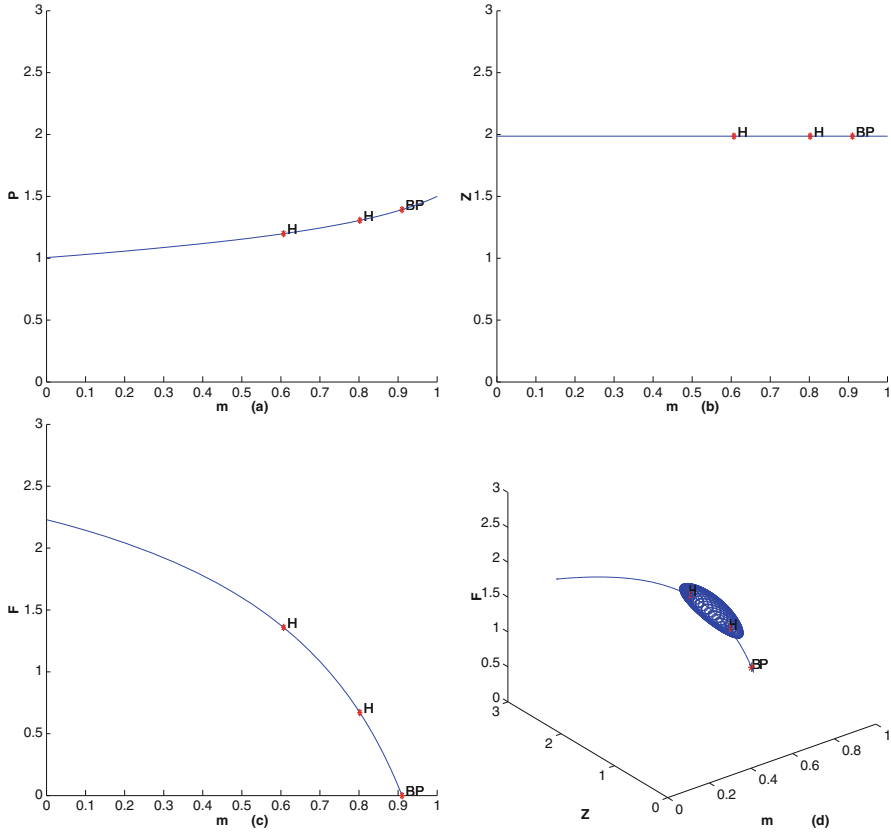Hopf points is plotted (cf. Fig. 4d).

Fig. 3 (a) The figure depicts different steady-state behaviors of phytoplankton for the effect of m. (b) The figure depicts different steady-state behaviors of zooplankton for the effect of m. (c) The figure depicts different steady-state behaviors of fish for the effect of m. (d) The family of limit cycles bifurcate from the Hopf point H for m in (m,Z,F) space

5.4 Effects of h

To study the impact of harvesting on fish population we vary the parameter h. We note that the system (1) has one Hopf point at 0.1484 with first Lyapunov coefficient being $1.059854e^{+01}$ one limit point at 0.1486 and branch point at 0.1468 (cf. Fig. 5a). We have drawn a family of unstable limit cycles bifurcating from H points (cf. Fig. 5b).
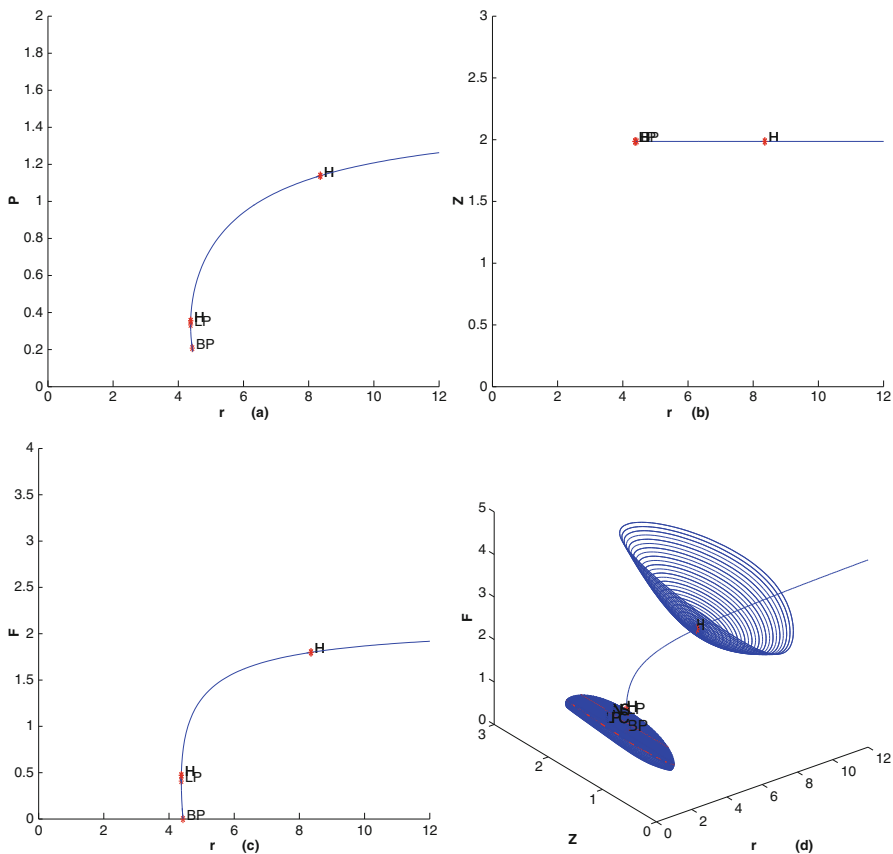
Fig. 4 (**a**) The figure depicts different steady-state behaviors of phytoplankton for the effect of r. (**b**) The figure depicts different steady-state behaviors of zooplankton for the effect of r. (**c**) The figure depicts different steady-state behaviors of fish for the effect of r. (**d**) The family of limit cycles bifurcate from the Hopf point H for r in (r,Z,F) space

5.5 *Hopf-Bifurcation*

For clear understanding of a dynamic change due to change in n, m and r, we have plotted three bifurcation diagrams separately (cf. Fig. 6a–c). Next, we have plotted two parameter bifurcation diagrams for $n-m$, $n-r$ and $m-r$ respectively (Figs. 7a–c) to show the stable zone at E^*. All the numerical results are summarized in Table 2.
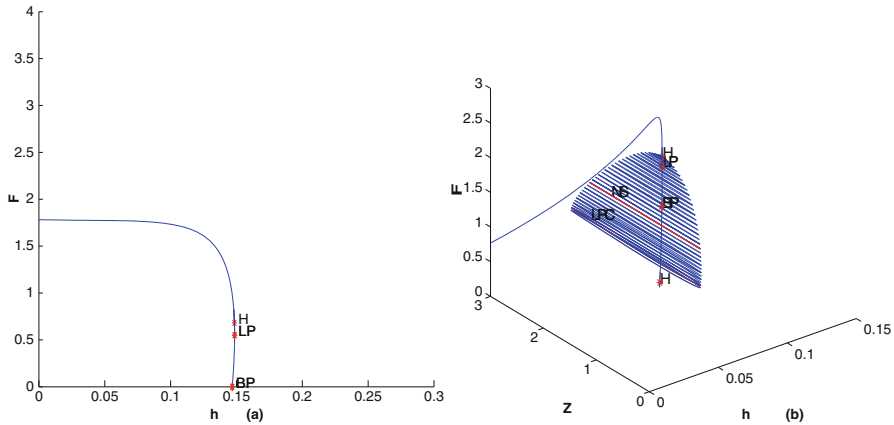
Fig. 5 (**a**) The figure depicts different steady-state behaviors of fish for the effect of h. (**b**) The family of limit cycles bifurcate from the Hopf point H for r in (r,Z,F) space

Table 2 Natures of equilibrium points

Parameters	Values	Eigenvalues	Equilibrium points
n	0.321158	$(-4.81561, \pm 0.404804i)$	Hopf (H)
	0.644284	$(-.0007, \pm 1.39674i)$	Hopf (H)
	0.644318	$((0, \pm 1.39308i)$	Limit Point (LP)
	0.640187	$(0, 0.13333 \pm 1.27889i)$	Branch Point (BP)
m	0.606983	$(5.50548, \pm 0.350157i)$	Hopf (H)
	0.802120	$(-6.55763, \pm 0.244601i)$	Hopf (H)
	0.910270	$(-7.29689, -0.0187574, 0)$	Branch Point (BP)
r	8.357091	$(-5.0378, \pm 0.404562i)$	Hopf (H)
	04.379199	$(-.00147, \pm 1.04446i)$	Branch Point (BP)
	4.377626	$(0, \pm 1.04446i)$	Limit Point (LP)
	4.428463	$(0, \pm 0.929514i)$	Branch Point (BP)
h	0.148487	$(-0.001428, \pm 1.39158i)$	Hopf (H)
	0.148622	$(0, 0.04471 \pm 1.38661i)$	Limit Point (LP)
	0.146818	$(0, 0.13453 \pm 1.26379i)$	Limit Point (LP)

5.6 *Environmental Fluctuations*

Next, we examine the dynamical behavior of the system in the presence of environmental disturbances. We apply the Euler-Maruyama method and investigate the stochastic differential equation numerically using MATLAB.

Firstly, we satisfy the conditions for asymptotic stability at E^* according to the mean square sense which depends on system parameters of (12) and σ_1, σ_2, σ_3. Taking $\sigma_1 = 0.1$, $\sigma_2 = 0.1$, $\sigma_3 = 0.1$, the values of intensities of the environmental perturbations with reference set of parametric values as in Table 1 for which all
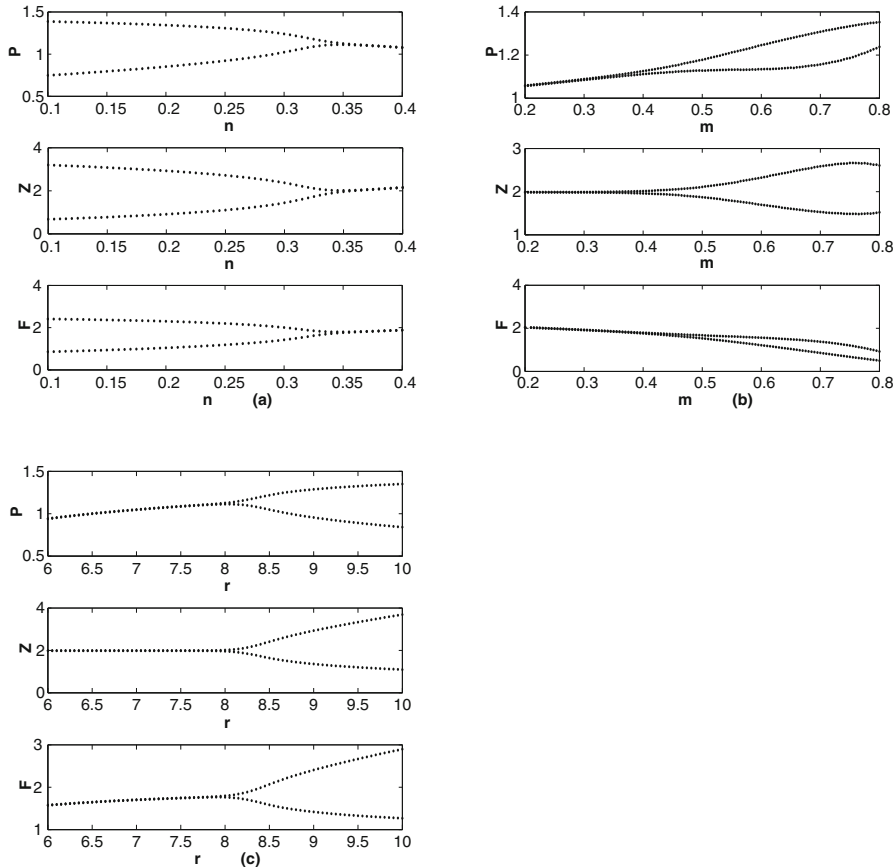
Fig. 6 (**a**) The bifurcation diagram for *n*. (**b**) The bifurcation diagram for *m*. (**c**) The bifurcation diagram for *r*

the three species coexist and the system is stochastically stable (cf. Fig. 8a). But it is clearly indicates that the coexistence equilibrium becomes unstable for higher values of intensities of the environmental perturbations, $\sigma_1 = 0.8$, $\sigma_2 = 0.8$, $\sigma_3 = 0.7$ (cf. Fig. 8b).

6 Discussion

We have formulated a mathematical model sketching the interaction of phytoplankton-zooplankton-fish species. The main focus is on the functional response in presence of refuge effects of phytoplankton and zooplankton on the marine ecosystem. The model parameters are also analysed by either varying one of them or combining some of them.
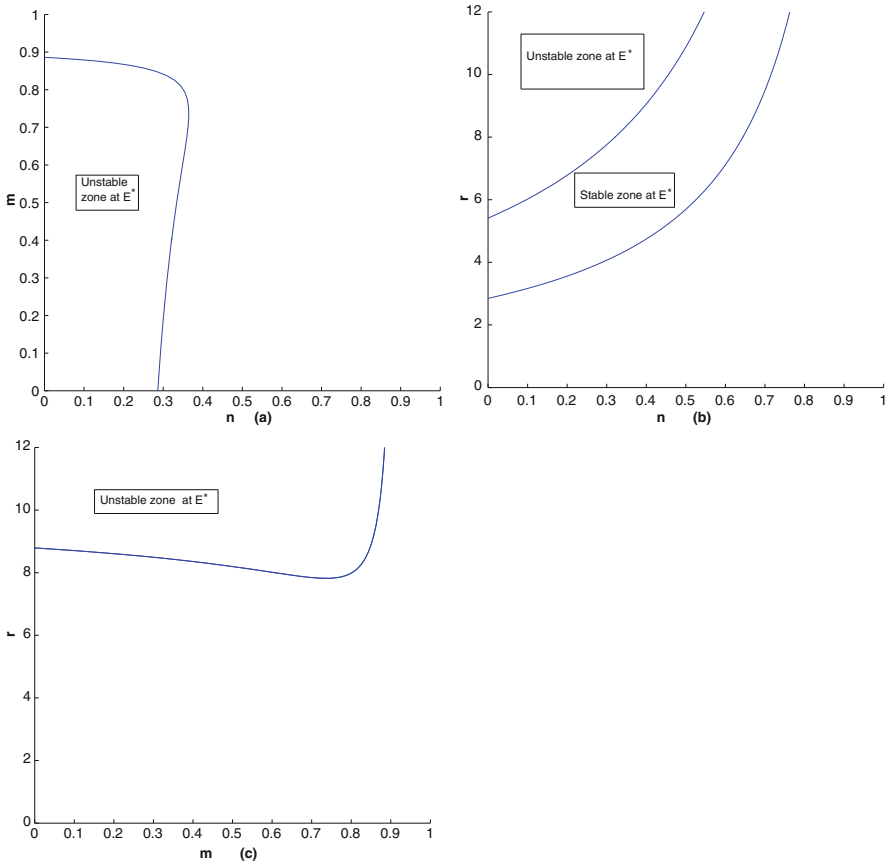
Fig. 7 (**a**) The two parameters bifurcation diagram for $n - m$. (**b**) The two parameters bifurcation diagram for $n - r$. (**c**) The two parameters bifurcation diagram for $m - r$

The stability of the three possible steady states namely plankton-free, the zooplankton-free and the coexistence equilibria are determined by studying the model analytically. The equilibrium states are observed to be related by transcritical bifurcations provided the parameter values matches suitable conditions. Hopf bifurcation at the coexistence equilibrium are obtained after analytical results and are backed by the numerical simulations. By changing the various parameters, persistent oscillations occur.

Numerically, oscillation of all population is observed when we reduce the strength of phytoplankton refuge and when the strength of zooplankton is increased. Further, same results are obtained by increasing the constant intrinsic growth rate of phytoplankton. The whole system is stabilized by harvesting rate of fish which plays a crucial role in marine ecosystem.
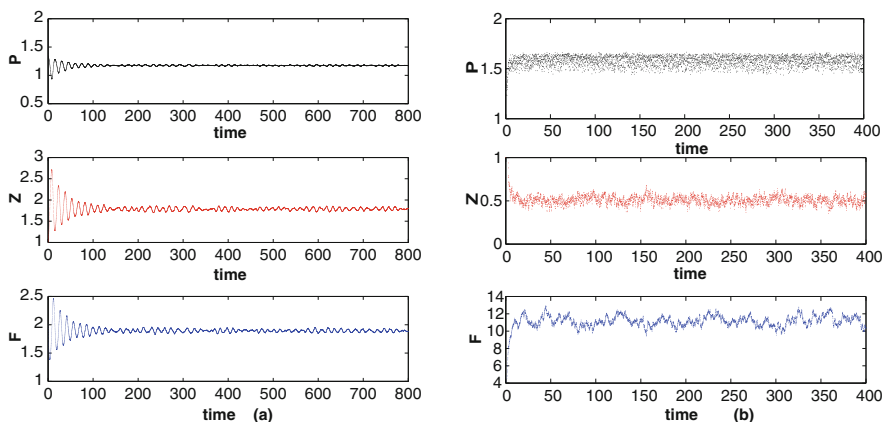
Fig. 8 (a) The figures depicts solution of system is stochastically stable for $\sigma_1 = 0.1, \sigma_2 = 0.1$ and $\sigma_3 = 0.1$. (b) The figures depicts solution of system is stochastically unstable for $\sigma_1 = 0.8, \sigma_2 = 0.8$ and $\sigma_3 = 0.7$

Based on the results,we can conclude that the strength of phytoplankton and zooplankton refuge, intrinsic growth rate of phytoplankton and harvesting rate of fish should be maintained within a range in order to avoid extinction of fish and recurrence bloom.

Environmental noise is further added to the model and it's low intensities makes the system stochastic asymptotic stable. High intensity values result in oscillations with high amplitudes. The model becomes stochastically stable if it fulfills certain conditions involving the maximum size of the environmental random fluctuations and the model parameters.

References

1. S. Khajanchi and S. Banerjee, Role of constant prey refuge on stage structure predator–prey model with ratio dependent functional response. *Applied Mathematics and Computation* **314**, 193–198 (2017).
2. X. Xie, Y. Xue, J. Chen and T. Li, Permanence and global attractivity of a nonautonomous modified Leslie-Gower predator-prey model with Holling-type II schemes and a prey refuge. *Advances in Difference Equations* **2016(1)**, 1–11 (2016).
3. S. Khajanchi and S. Banerjee, Role of constant prey refuge on stage structure predator–prey model with ratio dependent functional response. *Applied Mathematics and Computation* **314**, 193–198 (2017).
4. M. Haque, S. Rahman, E. Venturino and B. L. Li, Effect of a functional response-dependent prey refuge in a predator–prey model. *Ecological Complexity* **20**, 248–256 (2014).
5. D. Jana and S. Ray, Impact of physical and behavioral prey refuge on the stability and bifurcation of Gause type Filippov prey-predator system. *Modeling Earth Systems and Environment*, **2(1)**, 24 (2016) https://doi.org/10.1007/s40808-016-0077-y.

6. A. Das and G. P. Samanta, A prey-predator model with refuge for prey and additional food for predator in a fluctuating environment. *Physica A: Statistical Mechanics and its Applications* **538**, 122844 (2020).

7. W. Zhang and M. Zhao, Dynamical Complexity of a Spatial Phytoplankton-Zooplankton Model with an Alternative Prey and Refuge Effect. *Hindawi Publishing Corporation Journal of Applied Mathematics* Volume **2013**, Article ID 608073 (2013).

8. J. Li, Y. Song, H. Wan and H. Zhu, Dynamical analysis of a toxin-producing phytoplankton-zooplankton model with refuge. *Mathematical Biosciences and Engineering* **14(2)**, 529–557 (2017).

9. W. Sun, S. Dong, X. Zhao, Z. Jie, H. Zhang, and L. Zhang, Effects of zooplankton refuge on the growth of tilapia (Oreochromis niloticus) and plankton dynamics in pond. *Aquaculture international* **18(4)**, 647–655 (2010).

10. M. Bandyopadhyay and J. Chattopadhyay, Ratio-dependent predator-prey model: Effect of environmental fluctuation and stability. *Nonlinearity* **18** , 913–936 (2005).

11. T. Liao, C. Dai, H. Yu, Z. Ma, Q. Wang and M. Zhao, Dynamical analysis of a stochastic toxin-producing phytoplankton–fish system with harvesting. *Advances in Difference Equations* **2020(1)**, 1–22 (2020).

12. Z. Chen, S. Zhang and C. Wei, Dynamics of a stochastic phytoplankton-toxin phytoplankton–zooplankton model. *Advances in Difference Equations*, **2019(1)**, 1–18 (2019).

13. H. Liu, C. Dai, H. Yu, Q. Guo, J. Li, A. Hao, J. Kikuchi and M. Zhao, Dynamics induced by environmental stochasticity in a phytoplankton-zooplankton system with toxic phytoplankton. *Mathematical Biosciences and Engineering*, **18(4)**, 4101–4126 (2021).

14. W. W. Murdoch and J. Bence, General predators and unstable prey populations, in: Predation: direct and indirect impacts on aquatic communities. (W. C. Kerfoot and A. Sih, eds.), *University Press of New England*, Hanover, 17–30 (1987).

15. A. Chatterjee and S. Pal, Dynamical Analysis of Phytoplankton–Zooplankton Interaction Model by Using Deterministic and Stochastic Approach. In: Mondaini R.P. (eds) *Trends in Biomathematics: Chaos and Control in Epidemics, Ecosystems, and Cells. BIOMAT 2020.* Springer, Cham, 33–56 (2021).

16. P.K. Tapaswi and A. Mukhopadhyay, Effects of environmental fluctuation on plankton allelopathy, *J. Math. Biol.* 39, 39–58 (1999).

17. E. Beretta, V.B. Kolmanowskii and L. Shaikhet, Stability of epidemic model with time delays influenced by stochastic perturbations, *Math. Comp. Simul.* **45 (3-4)**, 269–277 (1998).

18. I.I. Gikhman and A.V. Skorokhod, The Theory of Stochastic Process-I, Springer, Berlin, (1979).

19. L. Shaikhet, Lyapunov Functionals and Stability of Stochastic Functional Differential Equations. Springer, Dordrecht, Heidelberg, New York, London, 2013.

20. V.N. Afanas'ev, V.B. Kolmanowskii and V.R. Nosov, Mathematical Theory of Control Systems Design, Kluwer Academic, Dordrecht, (1996).

21. M. Bandyopadhyay and J. Chattopadhyay, Ratio-dependent predator-prey model: Effect of environmental fluctuation and stability, *Nonlinearity* **18**, 913–936 (2005).

22. S. Pal and A. Chatterjee, Dynamics of the interaction of plankton and planktivorous fish with delay. *Cogent Mathematics* **2(1)**, 1074337 (2015).